Supplementary Material

for

The valence and Rydberg states of difluoromethane: a combined experimental vacuum ultraviolet spectrum absorption and theoretical study by *ab initio* configuration interaction and density functional computations.

Michael H. Palmer,[1,a] Søren Vrønning Hoffmann,[2,b] Nykola C. Jones,[2,b] Marcello Coreno,[3,b] Monica de Simone,[5,b] Cesare Grazioli,[4,b]

[1] *School of Chemistry, University of Edinburgh, Joseph Black Building, David Brewster Road, Edinburgh EH9 3FJ, Scotland, UK*

[2]*Department of Physics and Astronomy, ISA, Aarhus University, Ny Munkegade 120, DK-8000 Aarhus C, Denmark*

[3] *ISM-CNR, Montelibretti, c/o Laboratorio Elettra, Trieste, Italy*

[4] *CNR-IOM Laboratorio TASC, Trieste, Italy*

[a] Email: *m.h.palmer@ed.ac.uk*: Telephone: +44 (0) 131 650 4765

[b] *Electronic addresses: vronning@phys.au.dk; nykj@phys.au.dk; marcello.coreno@elettra.eu; desimone@iom.cnr.it; cesare.grazioli@elettra.eu;*

Contents

**SM9. The lowest singlet state of the 3-root CASSCF state-average calculation.**

SM10. Supplementary Material References.

SM1. The VUV 'subtraction' process.

Figure SM1 shows the VUV spectrum used, together with its treatment. A very wide Gaussian function, behaves similar to a ramp, is initially subtracted by use of a set of points touching the VUV curve at appropriate positions. A set of local Gaussian functions is then used in regions of interest to enhance the sharp structure, attributed to Rydberg and possibly valence states. The broad structure is inconsistent with Rydberg states both in style and high intensity, which generally contrasts with the sharp but weak Rydberg state appearance. The latter is expected to be similar to the photoelectron spectrum.

Figure SM1. The deconvolution process used.
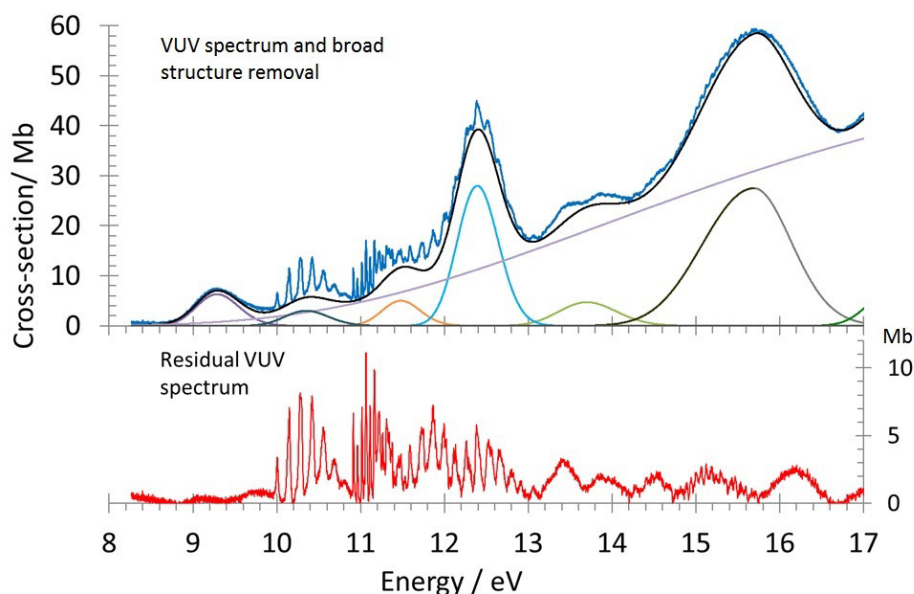
SM2. Computational methods expanded. Basis sets. Our results were mainly performed with the optimized Coulomb fitting (second) family of basis sets (DEF2),[27,28] where 'DEF' is an abbreviation for 'default'. Specifically, we used DEF2-QZVP (quadruple zeta valence with polarization) and DEF2-QZVPPD (which contains additional p- and d-diffuse functions). The aug-cc-pVQZ basis set contained [5s4p3d2f] contracted functions for the *H*-atoms, and [6s5p4d3f2g] for the *C* and *F* atoms, including diffuse functions. These will evaluate both the valence states and the lowest Rydberg states correctly; higher Rydberg states require very diffuse exponents, which we have previously used with the triple zeta

valence with polarization (TZVP) basis set.[1-4] Here a Rydberg set of functions [4s3p3d3f], was mounted on aug-cc-pVTZ as the background basis. However, this study also required bases showing a clear distinction between valence and Rydberg functions. The balance between basis set quality and bias towards either the ground state or the Rydberg state, has been extensively studied, and the above bases have been recommended for reliable results.[5-7]

SM3. Molecular orbital interactions in the excited states of CH_2F_2. The TDDFT method, in common with many related methods, defines the excitation energies (EE) and their associated oscillator strength (f(r)), as the difference in energy between the ground and the excited state, *at the same geometry*. When the equilibrium structures of the X^1A_1 and (say) X^1B_1 state are significantly different, these energies require correction to obtain the standard adiabatic value (AEE), in terms of the equilibrium structures of *both* states. The TDDFT procedure generates AEE low by 1 to 2 eV; for these two states, the EE (*G-09*) and AEE are 7.1468 and 8.7111 eV respectively.

SM4. Effect of symmetry and near degeneracy on the excited states. The TDDFT and CASSCF methods for calculation of singlet excited states, show mixing of MOs occurs in the leading terms of the wave-functions. These result in two complications; (a) separation into symmetric and antisymmetric combinations of same symmetry; (b) interaction of states of different symmetry in near degenerate situations. Thus, the onset of absorption in the VUV arises from a nearly degenerate pair of states, 1^1A_2 and 1^1B_1, both in the TDDFT and CASSCF methods. Analysis of Band I of the VUV spectrum is made more complex by both these interactions. Important examples, of particular relevance to the VUV Band I, are 1^1B_1 with 2^1B_1 and also 1^1A_2 with 2^1A_2. These states have leading terms:

1^1B_1: $2b_17a_1* - 2b_18a_1* - 2b_19a_1*$
2^1B_1: $2b_17a_1* + 2b_18a_1* + 2b_19a_1*$
1^1A_2: $2b_15b_2* - 2b_16b_2* - 2b_17b_2*$
2^1A_2: $2b_15b_2* + 2b_16b_2* + 2b_17b_2*$

We have studied the potential energy surfaces (PotEnergy) of these same state symmetry interactions by TDDFT methods. It is convenient to use a CH_2F_2 structural parameter, angle or bond, to exhibit this. Examples are shown in Figs SM2.1 and SM2.2, where the FCF angle was appropriate. A PotEnergy scan of the lowest state of symmetry (1^1B_1 etc) towards the next higher state (2^1B_1 etc) of same symmetry, shows the PotEnergy of both states. However, when these two states are similarly scanned in the opposite direction, ie starting with 2^1B_1 and scanning towards 1^1B_1, the curves are not identical. The surface exhibits hysteresis, where the region between them is different when the surface is scanned from the higher AEE state to the lower AEE state.

Figure SM4.1. The potential energy surface for the antisymmetric combination of the 1^1A_2 and 1^1B_1 singlet states. This was determined by use of state-averaged CASSCF calculations, using the TZVP basis set with 8 electrons in 8 MOs. The curve gives a close fit to a cubic equation.
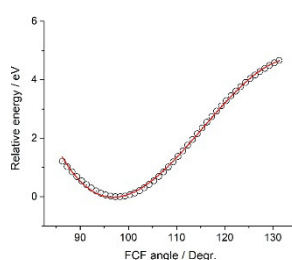
In contrast to the TDDFT program, part of *G-09*, the 'State Average' option in CASSCF calculations, allows mixing of configurations of differing symmetry. This became important, when additional mixing of 1^1B_1 and 2^1B_1, with 1^1A_2 and 2^1A_2 states became apparent. The surface for the lowest singlet 1^1B_1 and 1^1A_2 valence state are close through much of the attractive range, but cross for an FCF angle of 110.5°.

SM5. Position of Rydberg state functions. MCSCF calculations were performed where the Rydberg S-type functions were placed on either the ***C***- or both ***H***-, or both ***F***-atoms. Eighteen electrons were processed in 24200 determinants, covering three states of $^1A_1$ symmetry. The equilibrium structures were obtained for the lowest S- and P-Rydberg states, 1^1B_1 and 1^1A_1. The choice of placing the Rydberg state functions on the H-atoms gave structures very close to that for the X^2B_1 state and close to the X^1A_1 state under the same conditions, as shown in Table SM2.3. The alternative choice of the F-atoms gave a much

longer C-F bond, and larger HCF angle. Placing the Rydberg functions on the C-atom did not give a realistic structure, since both **C-H** and **C-F** bonds were lengthened to 1.4 Å and the **HCF** angle was reduced to 62°. Overall, the choice of Rydberg functions on the H-atoms seems appropriate. Similar conclusions were found in application to the Rydberg 3S state in **CHF₃**. This supports the views of Edwards and Raymonda that the lowest excited state arises from excitation of the **C-H** bond.[8]

Table SM5.1. Rydberg state energies and equilibrium structures, using the MCSCF method using the TZVP basis set, augmented by the Rydberg basis set placed on each H-atom.

Rydberg state	X^1B_1	$^1B_1$	$^1B_1$	$^1A_1$
Occupancy	$2b_13S^b$	$2b_14s$	$2b_13p$	$2b_13p$
Adiabatic IE / eV	8.6732	9.1317	7.9265	8.9933
C-H bond /Å	1.1600	1.1391	1.1712	1.1420
C-F bond/ Å	1.3178	1.3291	1.3345	1.3310
HCH angle/°	83.70	96.2265	87.8641	99.3940
FCF angle/°	121.93	115.1406	113.9785	114.9951
HCF angle/°	111.19			

Footnotes to Table SM5.1

   a. MCSCF X^1A_1 occupancy for a_1, b_1, b_2, a_2 orbitals as: [2200, 220, 220, 20] respectively. Number of configuration state functions (CSFs) 42746, generating 157016 determinants.
   b. Leading terms [22α0, 2β0, 220, 20]

SM6. Conical intersections and avoided crossings. The CASSCF module within the *G-09* suite, determines the position of closest energy approach for two states, while sharing a common structure. An avoided crossing or conical interaction (Conint), is determined by inspection of the wave-function at the common point. We have checked whether an avoided crossing or a conical interaction occurs between the two states 1^1B_1 and 2^1B_1, since a Conint would cause major perturbation to the vibrational levels. The **C-H** bond length provides a suitable variable for these potential energy surfaces of **CH₂F₂**. The surface in Fig. SM2.2, shows a crossing of the two nearly touching curves, but only when the molecular parameters

have **C-H** 1.204, **C-F** 1.380 (Å) with **HCH** 67.1° and **FCF** 110.5°. These geometric

parameters are distant from the minima, and cannot influence the vibrational

Figure SM6.1. The pair of mixed 1^1A_2 and 1^1B_1 singlet states in symmetric and antisymmetric linear combinations, near the curve crossing. The method used is CASSCF state-averaged method for conical interactions. The relative energy scale is arbitrary, but expresses the individual separations of the second and third states from the ground state (root one). The parameters at the crossing are shown, are not greatly different from the equilibrium structures.
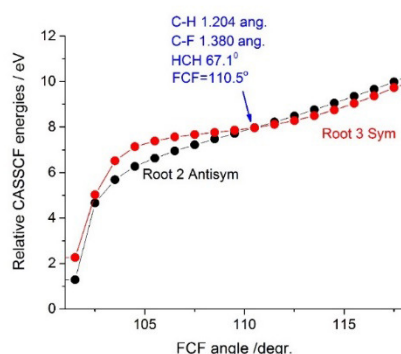
SM7. Singlet Rydberg states for CH_2F_2 using the MRD-CI method

Figure SM7. The VUV spectrum of CH_2F_2, with the MRD-CI vertical excitation energies with their oscillator strengths for the Rydberg states. These states generally show very low f(r), necessitating a separation from the valence state results.
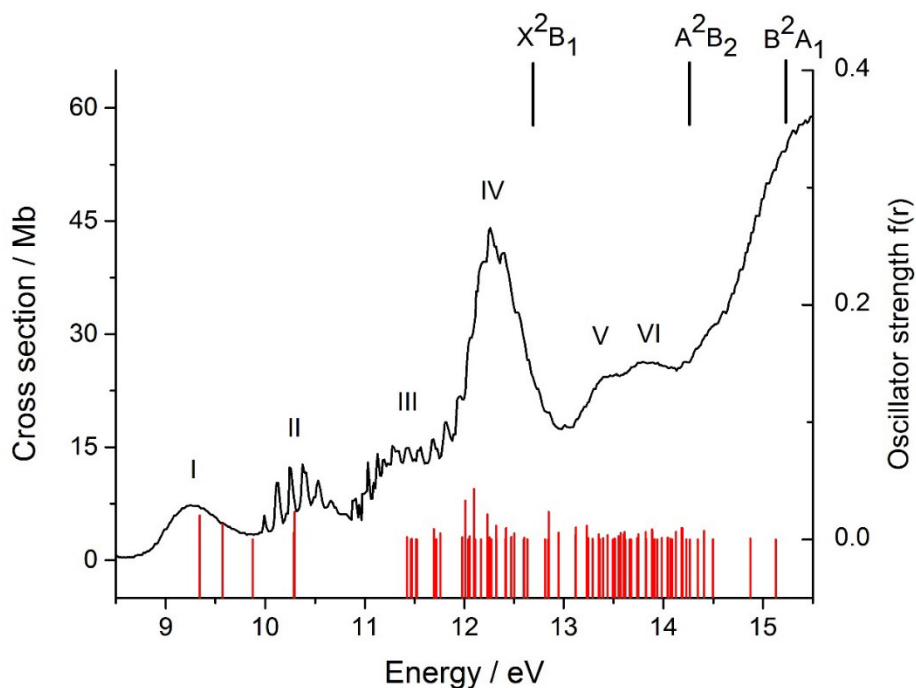
Table SM7. Selected vertical excitation energies (eV), including the leading configurations and second moments of the charge distribution (a.u.^{2})

Energy / eV	f(r)	Symmetry	Leading configurations	$\langle x^2 \rangle$	$\langle y^2 \rangle$	$\langle z^2 \rangle$
0.0	0.0	X^{1}A$_1$	1-4a$_1^2$;1-2b$_1^2$;1-3b$_2^2$;1a$_2^2$	-11.6	-14.2	-11.7
9.508523	0.024374	^{1}B$_1$	5,7-48	-27.5	-23.6	-29.0
10.393685	0.010825	^{1}B$_1$	6,10-48	-19.5	-19.8	-31.9
10.597752	0.029042	^{1}A$_1$	2b$_1$3b$_1$*	-42.3	-21.3	-23.7
11.773351	0.016653	^{1}B$_2$	6,5-82	-24.7	-22.1	-20.9
11.946601	0.001116	^{1}A$_1$	4a$_1$5a$_1$*	-28.5	-23.6	-23.8
12.103246	0.084329	^{1}B$_1$	7,8,13-48	-28.4	-24.0	-25.8
12.635757	0.098573	^{1}A$_1$	4a$_1$6a$_1$*	-19.9	-19.5	-37.2
12.695239	0.061053	^{1}B$_2$	4-83	-20.8	-32.2	-20.6
12.814916	0.039164	^{1}B$_1$	83-113;8-48	-22.5	-33.8	-22.5
13.139852	0.080144	^{1}A$_1$	2b$_1$5b$_1$*	-34.6	-19.3	-23.9
14.457600	0.049249	^{1}B$_1$	4-50,49	-49.9	-21.4	-34.3
14.800230	0.029188	^{1}B$_1$	11-48	-18.3	-28.7	-21.5
15.140321	0.063894	^{1}B$_2$	48-115;51-113	-27.4	-25.7	-24.4
15.370028	0.079545	^{1}B$_2$	9,8-82	-19.0	-31.7	-21.0
15.676760	0.036868	^{1}B$_2$	51-113;48-115	-33.6	-19.4	-27.9
15.868615	0.059742	^{1}A$_1$	3a$_1$5a$_1$* + 3b$_2$6b$_2$* +2b$_1$8b$_1$*	-23.9	-27.7	-26.5
16.001486	0.047647	^{1}B$_1$	12-48	-20.8	-17.9	-25.9
16.067505	0.049530	^{1}B$_1$	13-48;84-113	-29.0	-27.6	-28.1
16.154915	0.063668	^{1}B$_2$	6-81;10-82	-21.5	-21.0	-37.6
16.402301	0.050807	^{1}B$_2$	10-82;6-81	-22.4	-23.7	-33.2
16.469211	0.095619	^{1}A$_1$	4a$_1$10a$_1$* - 4a$_1$9a$_1$*	-22.0	-23.1	-34.2

[a] SCF energy -237.99596 a.u.; orbital occupancy 1a$_1^2$ - 6a$_1^2$, 1b$_1^2$ -2b$_1^2$, 1b$_2^2$ – 4b$_2^2$, 1a$_2^2$

[b] Excitation energies are relative to the $\widetilde{X}$ ^{1}A$_1$ ground state CI energy -238.39826 a.u

[c] Singly occupied orbitals except where shown; 97 active orbitals.

**SM8. The harmonic frequencies for the singlet states studied.**

Table SM8. Comparison of the vibrational modes (1 to 9) and harmonic frequencies (cm^{-1}) for the lowest singlet states with the X^{1}A$_1$ state and the Rydberg state ionic core X^{2}B$_1$.

State	X^{1}A$_1$	X^{2}B$_1$	1^{1}A$_2$	1^{1}B$_1$	2^{1}B$_1$	1^{1}A$_1$	2^{1}A$_1$	1^{1}B$_2$	3^{1}B$_1$	3^{1}A$_1$	4^{1}A$_1$	4^{1}B$_1$
1a$_1$	3100	2514	3158	2198	2588	2402	2355	2923	2450	2684	2704	2589
2a$_1$	1570	1292	1187	1289	1131	1286	1281	1180	1194	1450	1391	1376
3a$_1$	1150	1096	660	782	1021	1033	1059	1090	767	116	1041	1149
4a$_1$	540	604	271	562	262	607	603	485	545	468	461	560
5a$_2$	1297	997	401	1037	1063	1146	1206	1062	1029	1120	1177	1026
6b$_1$	3172	2069	3346	1892	2181	2089	2052	3068	2204	3085	3180	2198
7b$_1$	1207	618	594	747	-622	887	1119	1112	-840	883	944	351
8b$_2$	1486	1512	553	1486	1249	1476	1471	1477	1308	1167	1189	1374
9b$_2$	1143	1085	-5935	855	411	1076	1064	805	942	-1473	-1446	1235

SM9. The lowest singlet state of the 3-root CASSCF state-average calculation.

The lower singlet state, shown in Fig. SM8, gives a close fit to a cubic surface, and this is marked in red.

Figure SM9. The potential energy surface for the lowest mixed (1^{1}A$_2$ - 1^{1}B$_1$) state using state-averaged CASSCF calculations, and the TZVP basis set with 8 electrons in 8 MOs. The curve gives a close fit (shown in red) to a cubic equation. The derived frequencies show more low frequency modes than the ^{1}B$_1$ state in isolation, and this will lead both to a high density of states, and the more closely spaced vibraitonal separations shown in Fig.4 above.
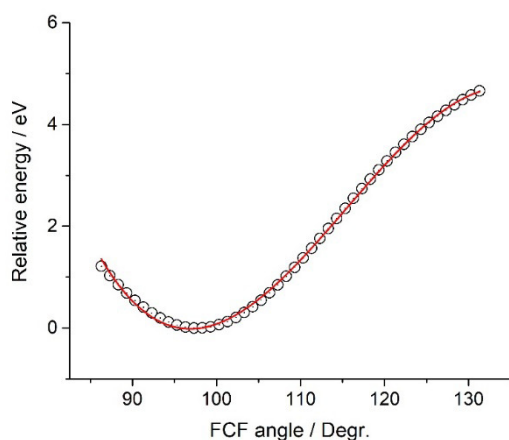
SM10. Supplementary Material References.

1. T. H. Dunning, J. Chem. Phys. **55**, 716 (1971)

2. A.D. McLean and G.S. Chandler, J. Chem. Phys. **72**, 5639 (1980).

3. D. E. Woon, and T. H. Dunning, J. Chem. Phys., **100**, 2975 (1994). Gaussian basis sets for use in correlated molecular calculations. IV. Calculation of static electrical response properties

4. M. H. Palmer, S. Vrønning Hoffmann, N. C. Jones, A.R. Head, D. L. Lichtenberger, J. Chem. Phys. **134**, 084309/1-084309/13 (2011)

5. D. Rappoport, ChemPhysChem , **12**, 3404 (2011).

6. D. Rappoport, N. R. M. Crawford, F. Furche, and K. Burk, 'Which functional should I choose?' in 'Computational Inorganic and Bioinorganic Chemistry.' Edited by Edward I. Solomon, Robert A. Scott, and R. Bruce King. John Wiley & Sons, Ltd: Chichester. UK, 2009. 594 pp. ISBN 978-0-470-69997-3. www.chem.uci.edu/~kieron/dft/pubs/RCFB08.pdf; viewed 4th December 2017.

7. J. A. Larsson, L. Tong, T. Cheng, M. Nolan, and J. C. Greer, J. Chem. Phys., **114**, 15 (2001) Estimating full configuration interaction limits from a Monte Carlo selection of the expansion space.

8. L. Edwards and J. W. Raymonda, J. Amer. Chem. Soc. **91**, 5937 (1969).